

LAPP-EXP-84-03
ISN -84-11
May 1984

Indication for neutrino oscillation
from a high statistics experiment
at the Bugey reactor

J.F.CAVAINAC, A.HOUMMADA, D.H.KOANG, B.VIGNON
Institut des Sciences Nucléaires de Grenoble, IN2P3,
38026 GRENOBLE CEDEX, France

and

Y.DECLAIS¹, H. de KERRET², H.PESSARD and J.M.THENARD
Laboratoire d'Annecy-le-Vieux de Physique des Particules, IN2P3,
Chemin de Bellevue, BP 909, 74019 ANNECY-LE-VIEUX CEDEX, France

Abstract

The energy spectrum of electron antineutrinos has been measured at two distances, 13.6 and 18.3 meters, from the core of a PWR power reactor at Bugey (FRANCE). About 63000 antineutrinos events have been recorded using the inverse β -decay reaction $\bar{\nu}_e + p \rightarrow n + e^+$. We observe a difference in the counting rates between the two positions. The compatibility of the results with solutions in a two-neutrino oscillation analysis is discussed.

- To be submitted to Physics Letters B -

¹ Now at Centre de Physique des Particules de Marseille, Faculté des Sciences de Luminy, Case 907, 70 Route Léon Lachamp, 13288 MARSEILLE CEDEX 9, France

² Now at Laboratoire de Physique Corpusculaire du Collège de France, 11 Place Marcelin-Berthelot, 75231 PARIS CEDEX 05, France

1. INTRODUCTION

Neutrinos oscillations are connected with the fundamental questions of neutrino mass and lepton number conservation. In a simple two-neutrino oscillation scheme, the probability of observing the same type of neutrino with energy E_ν at a distance L from a pure source is:

$$P(E_\nu, L, \theta, \delta m^2) = 1 - \sin^2 2\theta \times \sin^2(1.27 \times \delta m^2 [eV^2] \times \frac{L[m]}{E_\nu [MeV]})$$

where δm^2 is the difference of the squared masses of the two states of neutrinos, and θ is their mixing angle.

After Reines et al. publication on neutrino unstability in neutrino-deuterium data [Ref. 1], several dedicated experiments have been performed both at reactors [Refs. 2,3] and at accelerators [Refs. 4,5,6], bringing limits in δm^2 and $\sin^2 2\theta$ for ν_e and ν_μ oscillations.

We report here on an experiment performed at short distances from the core of a power reactor (2775 Mwth) at the Bugey (FRANCE) E.D.F. nuclear plant where the existence of foundation rafts allowed to set up a neutrino detector as close as 13.63 and 18.30 meters from the neutrino source. Very high statistics neutrino spectra have been recorded during a seventeen months data taking period to probe small neutrino mixings for a mass difference δm^2 in the range 0.1-4.0 eV^2 .

2. EXPERIMENTAL SET-UP

Nuclear reactors are pure sources of $\bar{\nu}_e$ which are emitted isotropically and originate from the beta-decay of fission products. In our case, the flux comes from a cylindrically shaped core (R=1.61m, H=3.66m) and is $2 \cdot 10^{13} / cm^2 / sec$ at 13.63m, which is the highest intensity presently available near a reactor.

The experimental area is completely isolated from the reactor core and associated activities by 2.5 meters of heavy concrete. The reactor structure and building provide a protection against cosmic rays of more than 25m water-equivalent. At the two distances (referred to as Position 1 and Position 2), we have built two identical cubic structures to shield the active detector. Each face of the cube consists, from inside to outside, of 7cm thick of low activity lead, 10cm of liquid scintillator (veto counters), 25cm of borated water and 10cm of lead. The veto counters, each viewed through WLS bars by one photomultiplier, are used to reject the cosmic muon induced events. The

two shielding doors and the active part of the detector are movable without disassembling, allowing position change within forty-eight hours.

Neutrinos are detected using the reaction $\bar{\nu}_e + p \rightarrow n + e^+$, and their energy given by $E_\nu = E_{e^+} + 1.8\text{MeV}$ (+ neutron recoil corrections). The detector [Ref. 7], similar to the one previously used at the ILL experiment [Ref. 2], is composed of 5 planes of 6 target cells, each filled with liquid scintillator (321 l total volume of NE235C, H/C=1.70, $\rho=0.861\text{ g/cm}^3$), sandwiched with four large He3 proportionnal chambers. The targets act as positron calorimeters and neutron moderators. Each cell is viewed by 4 phototubes recorded individually, allowing phototube noise rejection, and the signals are multiplexed in a way to avoid pile-up between targets. The neutrons, once thermalized, are captured in the neighbouring He3 chambers. A neutrino candidate is signed by a delayed coincidence between a positron and a neutron. Pulse shape discrimination techniques (PSD) applied to the target cells signals are used to reject events with a fast neutron induced by cosmic rays. The typical energy resolution is 20% FWHM at 1 MeV positron energy. The neutron detection efficiency map, measured over 204 points in the detector with a 1%-calibrated Sb-Be source, gives a mean efficiency value of $(26.18 \pm 0.88)\%$. Changes in the neutron efficiency due to a neutron orientation still linked to the neutrino incident direction, rather than an isotropic orientation, are included. Relative neutron detection efficiency and absolute energy calibration were measured periodically with radioactive neutron and gamma sources.

3. DATA TAKING

During the data taking, the single counting rates above the hardware thresholds, were typically 350/sec in the targets (mainly gammas) and 1.5/sec in He3 counters for neutrons. For the veto counters they were 155/sec at Position 1 and 176/sec at Position 2. All the single rates were independant of the reactor operation.

The deposited energy, timing and localisation of the neutron and of the three preceding gammas ($\gamma_1, \gamma_2, \gamma_3$) were written on magnetic tape as well as other relevant informations: reactor power, computer deadtime, veto flags of different durations (15, 498, 896, 1440 μsecs), and single rates from CAMAC scalars. The data recording was triggered by a neutron event satisfying He3 pulse-height threshold and veto criteria. In normal data taking, where the 498 μsecs length veto signal was included in the trigger, the trigger rate was 0.31/sec at both positions. Different data sets have been recorded from february 1982 to july 1983. The experimental conditions are defined in Table 1. The energy spectra of the two data sets measured at Position 1 are compared

in Fig. 1a. The good agreement demonstrates that all effects due to time variations of the energy calibration and apparatus stability have been well controlled over 17 months. At the second position, the reactor was operating at different powers. The integrated event rates between 1.5 and 6.5 MeV are plotted as a function of the reactor power in Fig 1b. The linearity, also observed in every energy bin, shows a correct control in particular of the effective time and reactor mean power. For an optimal use of all the information, we extract the positron energy spectrum for the second position from a linear fit of the four data sets available. The integrated event rates after background subtraction and renormalization to the same solid angle and number of fissions, are plotted for the different measurements as a function of the fuel mean burn-up in Fig. 1c.

Data Set	Pos1 A	Pos2 A	Pos2 B	Pos2 C	Pos2 OFF	Pos1 OFF	Pos1 B
Power (Mwth)	2755.8	2739.1	1636.4	2249.6	-	-	2782.7
Eff. time (hrs)	1197.6	1401.6	1103.7	623.5	529.2	738.5	936.4
Events/hour	28.27	15.38	10.78	13.43	3.87	3.91	28.57

(the events/hour rates are corrected for dead-time and losses, not for absolute neutron efficiency)

4. DATA ANALYSIS

To select neutrino events, the following criteria have been applied to the recorded data:

- neutron selection. A single He3 counter signal, in the neutron pulse-height window and no veto tag within 896 μ secs.
- positron selection. We define a good positron candidate as the first gamma signal with 4 phototube pulses matched, no 15 μ secs veto tag associated, only one target hit, and the corresponding energy deposition between 1.5 and 6.5 MeV.

Then the positron has to be correlated in space and time with the neutron: the target cell should be adjacent to the He3 counter and the time $t_{n\gamma}$ between neutron and positron signals smaller than 200 μ secs. From the observed $t_{n\gamma}$ distribution in the final sample, we get a correction factor to the neutron efficiency due to the $t_{n\gamma}$ cut of 0.792 ± 0.003 . Additional background subtraction is done by applying PSD cuts and imposing that the time between the

first and the second gamma, $t_{\gamma_1\gamma_2}$, is greater than 200 μsecs . The overall fraction of surviving events is 4.6% in Position 1 with reactor on.

The spectra, normalized in time, are also corrected for the dead times (data acquisition and veto counting) and for losses of events due to the PSD and $\gamma_1\gamma_2$ time cut. The overall correction is of the order of 20% depending on the data set.

In Table 1 are listed for each data set, the effective time and the neutrino events rates. After reactor off subtraction, we end up with 39881 ± 262 selected neutrino events in Position 1 for a mean reactor nuclear power of 2824 Mwth, and 23345 ± 310 in Position 2 for 2297 Mwth. The corresponding positron spectra are shown in Figs. 2a and 2b.

The expected positron spectra have been determined by a comprehensive Monte-Carlo simulation. The reactor geometry is fully detailed, the measured radial and longitudinal neutron density distributions are used. For each fuel assembly, the different contributions of the four fissile isotopes to the energy production were deduced from the daily state of burn-up provided by EDF [Ref. 8]. From this calculation, mean values are:

	U^{235}	U^{238}	Pu^{239}	Pu^{241}
Position 1	62.1%	7.6%	26.4%	3.9%
Position 2	47.9%	8.2%	36.9%	7.0%

For U^{235} and Pu^{239} , we take as input for the initial neutrino spectrum the measurements of Ref. 9. Among calculations giving results on the unmeasured U^{238} and Pu^{241} isotopes, we have used those of Ref. 10 which are in reasonable agreement with the measurements for U^{235} and Pu^{239} . Due to the low energy tail (edge effects) of the detector energy response and to our statistical significance in the high energy part of the spectrum (up to 8.3 MeV neutrino energies), we need to extrapolate the spectrum of each isotope from 8 to 10 MeV, using the Klapdor et al. calculations [Ref. 11] which extend up to 9 MeV. In the determination of the expected spectrum, we have separated in the errors on the initial spectrum, the normalization error (4.8%) from the point-to-point errors which affect the shape of the neutrino energy distribution. To calculate the positron spectrum, we apply the energy dependent cross-section,

$$\frac{d^2\sigma}{dE_{\bar{\nu}}}(\bar{\nu}_e p \rightarrow n e^+) = \frac{2\pi^2 h^3}{m_e^5 c^8 f \tau_n} [E_{\bar{\nu}} - (M_n - M_p)c^2] \left\{ [E_{\bar{\nu}} - (M_n - M_p)c^2]^2 - m_e^2 c^4 \right\}^{1/2}$$

where f is the phase space factor, corrected for radiative and weak magnetism effects according to Ref. 12. We use for the neutron lifetime $\tau_n = 900$ sec [Ref. 13]. The uncertainty on the cross-section from τ_n is taken as 2.0% reflecting the spread between the experimental measurements [Ref. 14]. Including the

error on the number of free protons (1.5%), on the neutron efficiency (3.4%), and on the monitoring of various cuts and corrections (2.6%), the overall normalization uncertainty is 6.9%.

We compute the energy response of the whole detector by folding in the spatial neutron efficiency with the complete simulation of the targets (neutrino interactions in lucite, cells edge effects, positron annihilations at rest and in flight, light collection). The kinematical correction to the measured neutrino energy due to the neutron recoil energy [Ref. 12] is included.

The expected positron spectra in the case of no oscillation for Position 1 and Position 2 are drawn in Figs. 2a and 2b together with the experimental spectra. The ratios $R = Y_{meas.}/Y_{expected}$ between measured and expected yields is shown for both positions in Figs. 3a and 3b. On Fig. 3c is the ratio R_{12} of Position 1 and Position 2 spectra corrected for the solid angle difference and changes due to the fuel composition as determined by the Monte-Carlo simulation.

5. RESULTS AND DISCUSSION

The ratio R for Position 1 is expected to be equal to one in case of no oscillation. Can the shape, statistically well defined with errors of about 2%/500keV bin, be explained by neutrino oscillations? There are large uncertainties on the expected spectrum. We have noted that choosing different initial neutrino spectrum calculations for the unmeasured U^{238} and Pu^{241} isotopes and different modes of extrapolation up to $E_{\bar{\nu}}=10$ MeV, lead to considerable distortions of the expected spectrum shape. To study these effects, we have used calculations of Kopeikin [Ref. 15] and of Klapdor et al. [Ref. 16]. In addition, a systematic shift of the order of 50 to 100 KeV is possible in the absolute energy calibration (in particular Compton scattering and bremsstrahlung could not be exactly simulated for our scintillator medium). Such shifts can lead to distortions of the same order on the spectrum shape. The uncertainties on the ratio R coming from these two effects are represented by the shaded area in Fig. 2a and, together with the large normalization error, preclude any definite conclusion.

With an experimental point-to-point error of about 4%/500keV bin, the shape of the ratio R for Position 2 is less compulsive by itself, and the same uncertainties on the expected spectrum also apply.

The Position 1/Position 2 ratio (Fig. 3c) is less dependant of the knowledge of the initial spectrum and of the other effects mentioned above. The integrated ratio of the positron experimental spectra between 1.5 and 6.5 MeV, corrected for the solid angle difference is $1.141 \pm 0.014_{stat.}$. The other correc-

tion to this ratio, due to the difference in the fuel isotopic composition, amount to 0.966 for our basic assumption (0.977 using Kopeikin, 0.958 using Klapdor et al. calculations). This leads to a corrected ratio of $1.102 \pm 0.014_{stat.} \pm 0.028_{syst.}$. The systematic error comes from:

a) stability of: detection (1.5%), thermal power of the reactor (1%) and cuts (1.5%)

b) differences in the evaluation of the effect of fuel isotopic composition changes (1.5%). This effect cannot explain the normalization difference with any choice of initial spectrum. Fig. 1c shows that a drastically different kind of variation would be needed. Such a sharp variation would correspond to a noticeable change in event rate between the beginning and the end of Position 1 measurements.

Could the difference with unity be explained by neutrino oscillations? From the Position 1/Position 2 ratio, we have two constraints, one coming from the shape, the other from the integrated counting difference. We define a chisquare for each constraint with:

$$R_{12}^i = \frac{Y_1^i}{Y_2^i}, \quad N_1 = \sum_{i=1}^{10} Y_1^i, \quad N_2 = \sum_{i=1}^{10} Y_2^i, \quad \text{and} \quad A = \left(\frac{N_1^{expect.}(\delta m^2, \theta)}{N_2^{expect.}(\delta m^2, \theta)} \right) / \left(\frac{N_1^{meas.}}{N_2^{meas.}} \right)$$

$$\chi_{Shape}^2 = \sum_{i=1}^{10} \left(\frac{A R_{12}^{i, meas.} - R_{12}^{i, expect.}(\delta m^2, \theta)}{A \sigma_{12}^{i, meas.}} \right)^2$$

$$\chi_{Norm.}^2 = \frac{\left(\frac{N_1^{meas.}}{N_2^{meas.}} - \frac{N_1^{expect.}(\delta m^2, \theta)}{N_2^{expect.}(\delta m^2, \theta)} \right)^2}{\sigma_{N_{12}}^2}$$

where $\sigma_{N_{12}}$ is the relative normalization error. These chisquares are not correlated and from their distributions in a large number of simulated experiments, we derive their 1, 2 and 3 σ probabilities. On Fig. 4 are shown the 2 and 3 σ contours for χ_{Shape}^2 in the $(\sin^2 2\theta, \delta m^2)$ plane. The no oscillation case is not excluded from the Position 1/Position 2 shape alone. The 2 and 3 σ contours for $\chi_{Norm.}^2$, also shown in Fig. 4, exclude the no-oscillation case at the 3 σ level and leave only two oscillation solution regions, one around $\delta m^2 = 0.8 \text{ eV}^2$, $\sin^2 2\theta = 0.12$, the other around $\delta m^2 = 0.2 \text{ eV}^2$, $\sin^2 2\theta = 0.25$. Combining the probabilities from the two kinds of contours, only the solution at 0.2 eV^2 is allowed, the other being above the 2 σ probability level.

We note that part of the solution region around $\delta m^2 = 0.2 \text{ eV}^2$ is not excluded by the two-position limits given by the Gösgen experiment [Ref. 3]. However, this solution does not fit very well with our single position ratios, R_1 and R_2 , even taking into account the possible distortions discussed at the beginning of

this chapter. The solution at 0.2 eV^2 is mainly constrained by the counting difference between the two positions. We have checked that no experimental effect in our present knowledge can explain this difference. The other solution at 0.8 eV^2 is more compatible with the single position ratios, but it accounts only partly for the counting rate difference.

6. CONCLUSION

We have accumulated high statistics neutrino spectra for the reaction $\bar{\nu}_e p \rightarrow n e^+$ at our two positions of detection. We cannot make use of the statistical accuracy to draw conclusions from the single position spectra but from the Position 1/Position 2 ratio, which is much less dependant of any systematic effect, we find indication of neutrino disappearance at the 3σ level. The integrated counting difference between the two positions is the main constraint in our results which can be explained in a simple two-neutrino oscillation scheme.

It would be important to confirm an oscillation effect with the single position spectra. Improvements in the determination of the expected neutrino spectrum could come from β -spectrum results on the fissile isotopes, specially for neutrino energies above 8 MeV. A better determination of the absolute detector response could also be achieved.

In the future, more precise relative measurements in the $\delta m^2 < 1 \text{ eV}^2$ range can be considered at reactors, in particular at the Bugey site.

Acknowledgements

The realization of this experiment has been possible only with the financial support of IN2P3 and EDF. We wish to thank the directors of IN2P3 and in particular Mr. J.Yoccoz for his continuous interest and encouragement to start up the experiment. We have benefited at Bugey from the efficient help of the EDF staff at all levels.

We thank our laboratories and their directors for their support and, in particular, we are grateful for the skillfull technical help of A.Bazan, C.Barnoux, B.Guerre-Chaley, M.L.Marmoux, G.Moynot, P.Mugnier, A.Oriboni, L.Pitrot, J.Thion and H.Vey.

We wish specially to thank G.Girardi whose active participation in all aspects of the experiment, during the end of the installation and a large part of the data taking period, has been much appreciated.

We acknowledge fruitful discussions with K.Schreckenbach, H.V.Klapdor and C Bastin.

References

- 1 : F.Reines et al., Phys. Rev. Lett. 45,(1980)1307.
- 2 : H.Kwon et al., Phys. Rev. D24,(1981)1097.
F.Boehm et al., Phys. Lett. 97B,(1980)310.
- 3 : J.L.Vuilleumier et al., Phys. Lett. 114B,(1982)298.
K.Gabathuler et al., Phys. Lett. 138B,(1984)449.
G.Zacek, Thesis TUM Munich Physics Dept. E15, February 1984.
- 4 : F.Dydak et al., CDHS Collab., Phys. Lett. 134B,(1984)281.
- 5 : F.Bergsma et al., CHARM Collab., CERN Preprint EP/84-36.
- 6 : C.Haber et al., CCFR Collab., FERMILAB Preprint CONF-83/57 Exp.
- 7 : A.Hoummada, Thèse 3eme cycle, ISN-82-27, July 1982.
- 8 : Calculations from "Division Calculs Nucleaires" of Electricité de France.
- 9 : K.Schreckenbach et al., Phys. Lett. 99B,(1981)251.
F. von Feilitzsch et al., Phys. Lett. 118B,(1982)162.
K.Schreckenbach ,Talk at the XIXth Rencontre de-Moriond (La Plagne, Jan. 84),
Preprint SP.84-42.
- 10 : P.Vogel et al., Phys. Rev. C24,(1981)1543.
- 11 : H.V.Klapdor et al., Phys. Rev. Lett. 48,(1982)127.
Phys. Lett. 112B,(1982)22.
- 12 : P.Vogel, CERN Preprint TH-3727.
- 13 : D.H.Wilkinson, Nucl.Phys. A377,(1982)474.
- 14 : C.J.Christensen et al., Phys. Rev. D5,(1972)1628.
L.N.Bondarenko et al., JETP Lett. 28,(1978)303.
J.Byrne et al., Phys. Lett. 92B,(1980)274.
D.H.Wilkinson, Prog. Rep. Nucl. Phys. 6,(1980)325.
- 15 : V.I.Kopeikin, Sov. J. Nucl. Phys. 32,(1980)1507.
- 16 : H.V.Klapdor and J.Metzinger, private communication of calculations on U^{238} and Pu^{241} .

Figure Captions

Fig. 1 :

- a). Ratio of the positron energy spectra measured at Position 1 at the beginning and at the end of the experiment, normalized to the same integrated power.
- b). Integrated event rates (between 1.5 and 6.5 MeV positron energies) measured at Position 2 versus reactor power.
- c). Background-subtracted event rates measured during the different data taking periods, normalized to the same solid angle and number of fissions, as a function of the fuel mean burn-up (in Megawatts-day/ton). The insert shows the stability of the event rate versus time during the Position 1 period, as an illustration of the lack of a strong variation which could explain the step in event rate between Position 1 and Position 2.

Fig. 2 :

- a). Positron energy spectrum measured at Position 1 (reactor OFF subtracted). The data points with dashed error bars show the reactor OFF spectrum. The error bars are statistical. The expected positron energy spectrum is shown as a shaded band delimited by the point-to-point errors.
- b). ditto at Position 2.

Fig. 3 :

- a). Ratio R_1 for Position 1 between measured and calculated event yields as a function of the positron energy. The shaded area shows the domain where the points move when different spectrum calculations are used for the U^{238} and Pu^{241} isotopes [Refs. 15,16] and when a systematic shift up to 100 KeV is applied to the absolute energy calibration.
- b). Ratio R_2 for Position 2 between measured and calculated event yields as a function of the positron energy.
- c). Ratio R_{12} between event yields measured at Position 1 and at Position 2 as a function of the positron energy, corrected for solid angle difference and fuel burn-up effect. The fuel burn-up correction is shown as a continuous line. The dashed lines show this correction when other calculations for U^{238} and Pu^{241} spectra are used [Refs. 15,16].

Fig. 4 :

Contours at 2 and 3 standard-deviations in the $(\sin^2(2\theta), \delta m^2)$ plane for χ_{Shape}^2 (dashed lines) and $\chi_{Norm.}^2$ (continuous lines). The areas not excluded at the 3σ combined probability level are shaded.

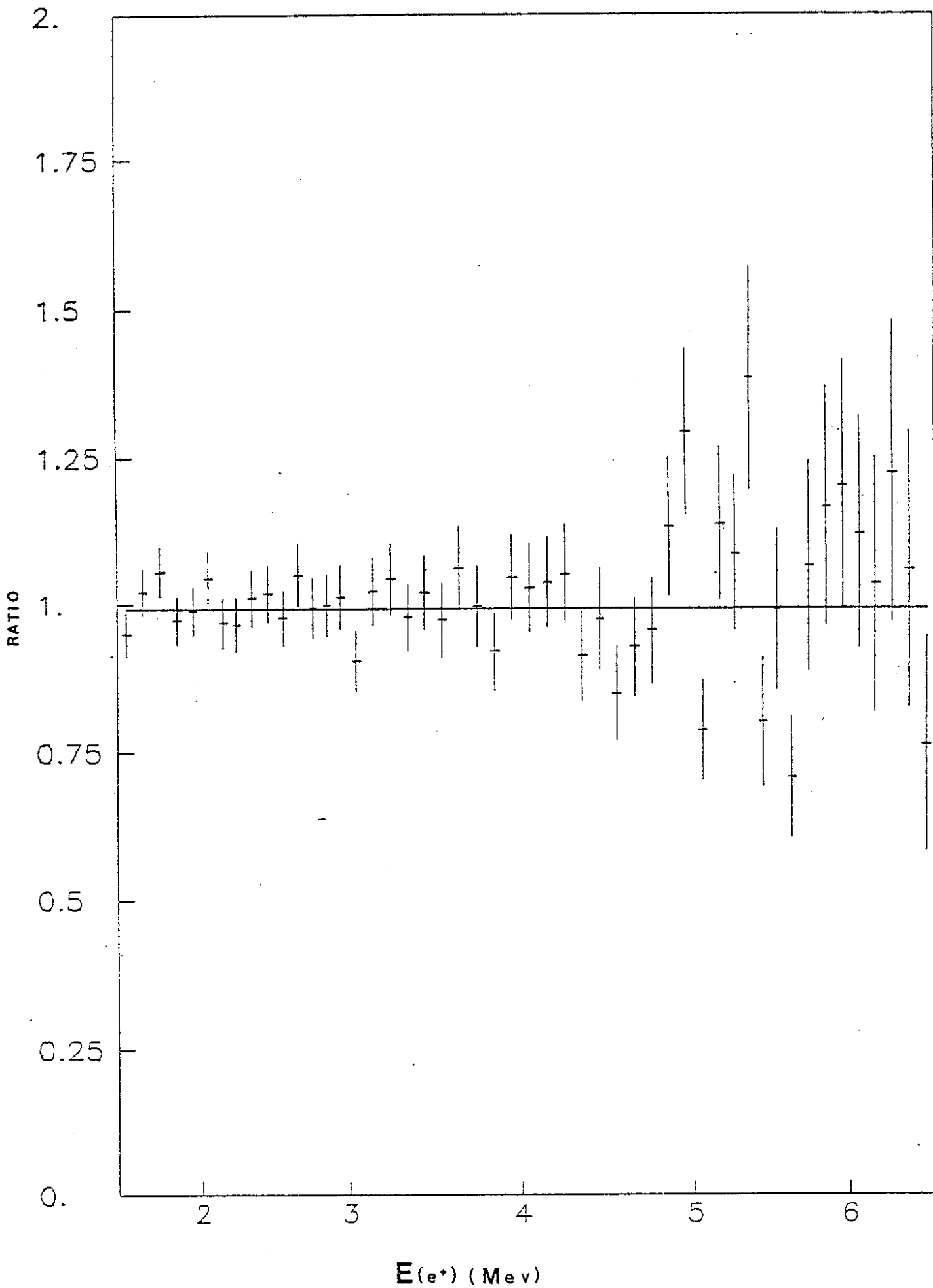
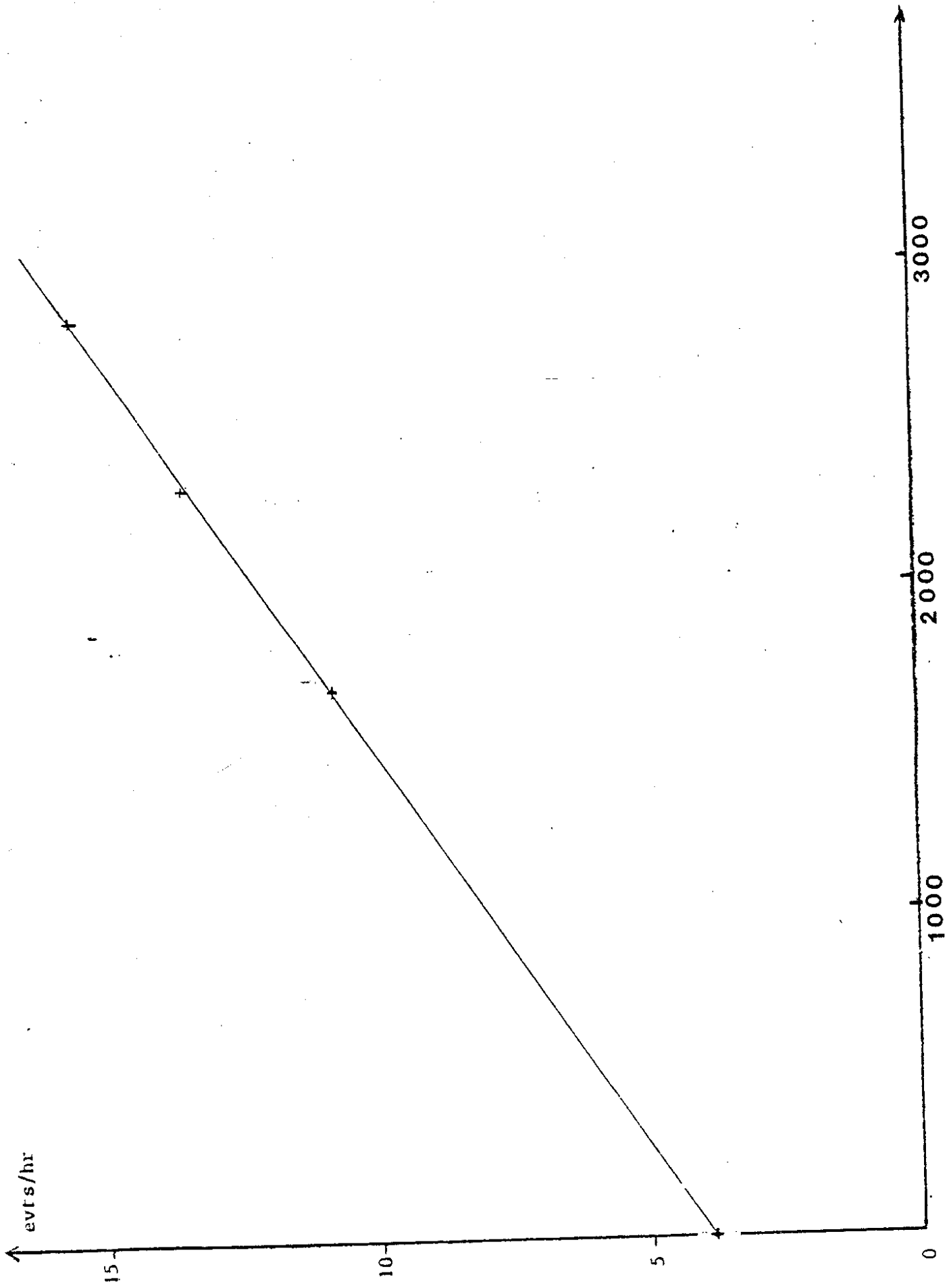


Figure 1A



POWER (MWh)

Figure 1B

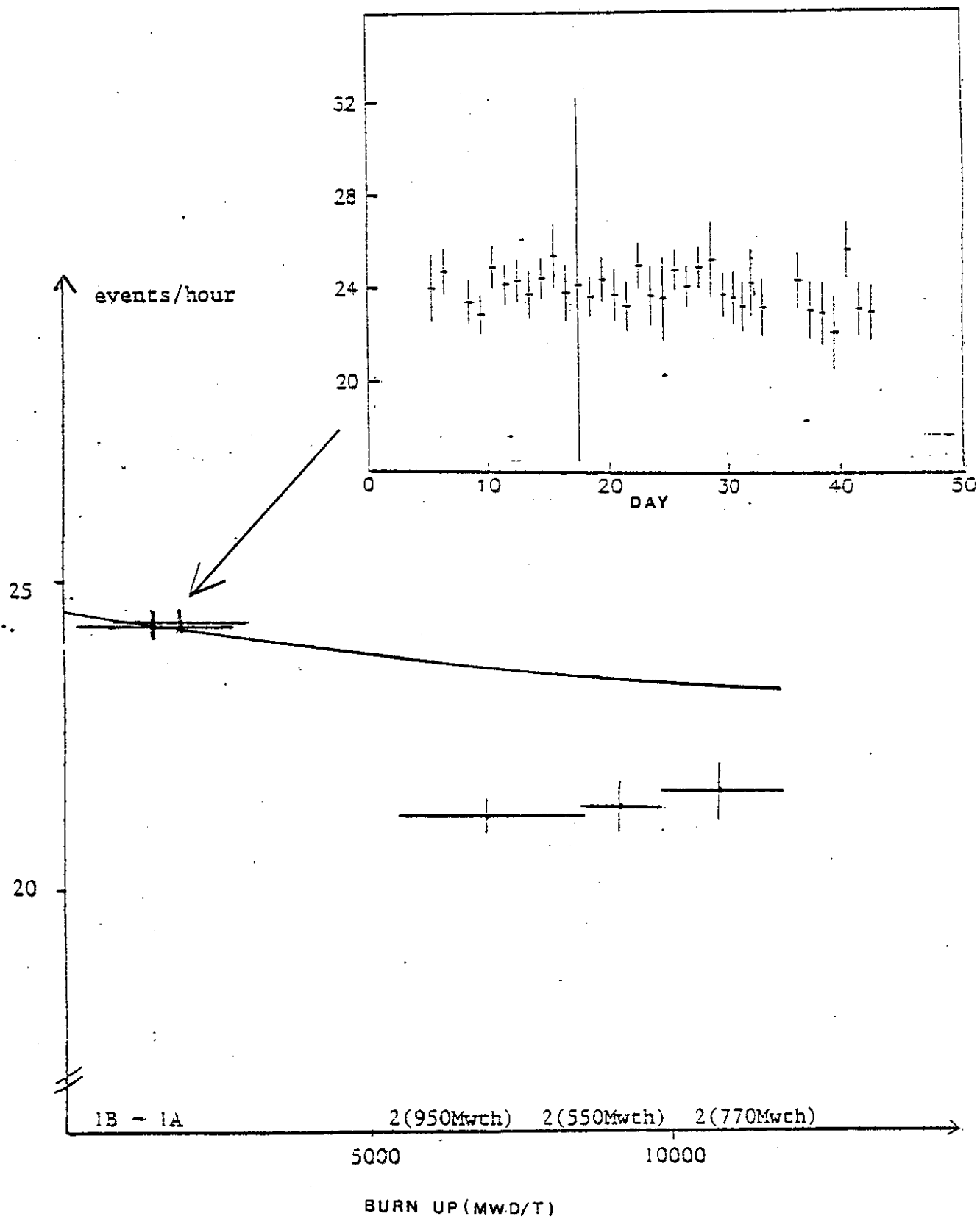
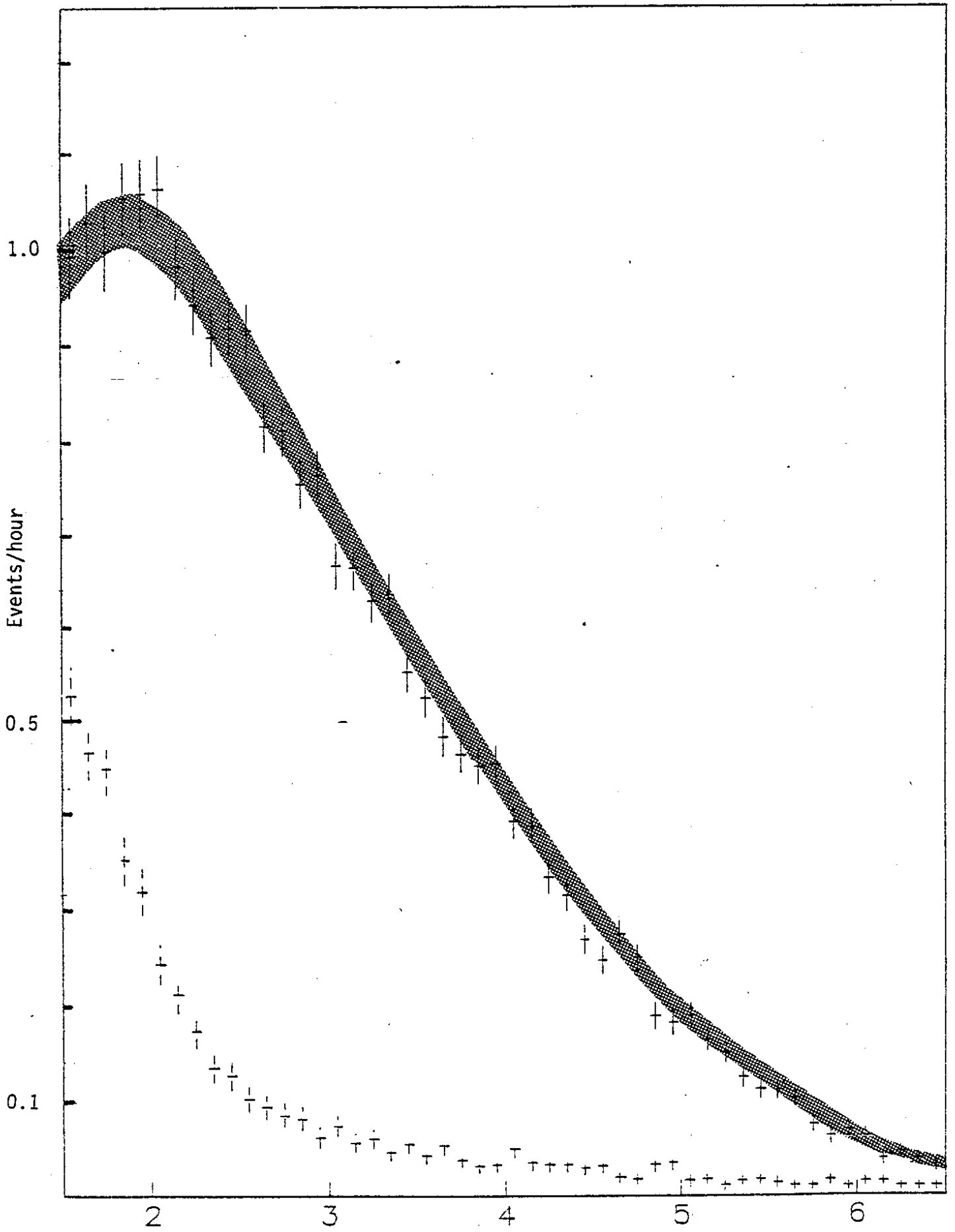


Figure 1C



$E(e^+)$ (Mev)

Figure 2A

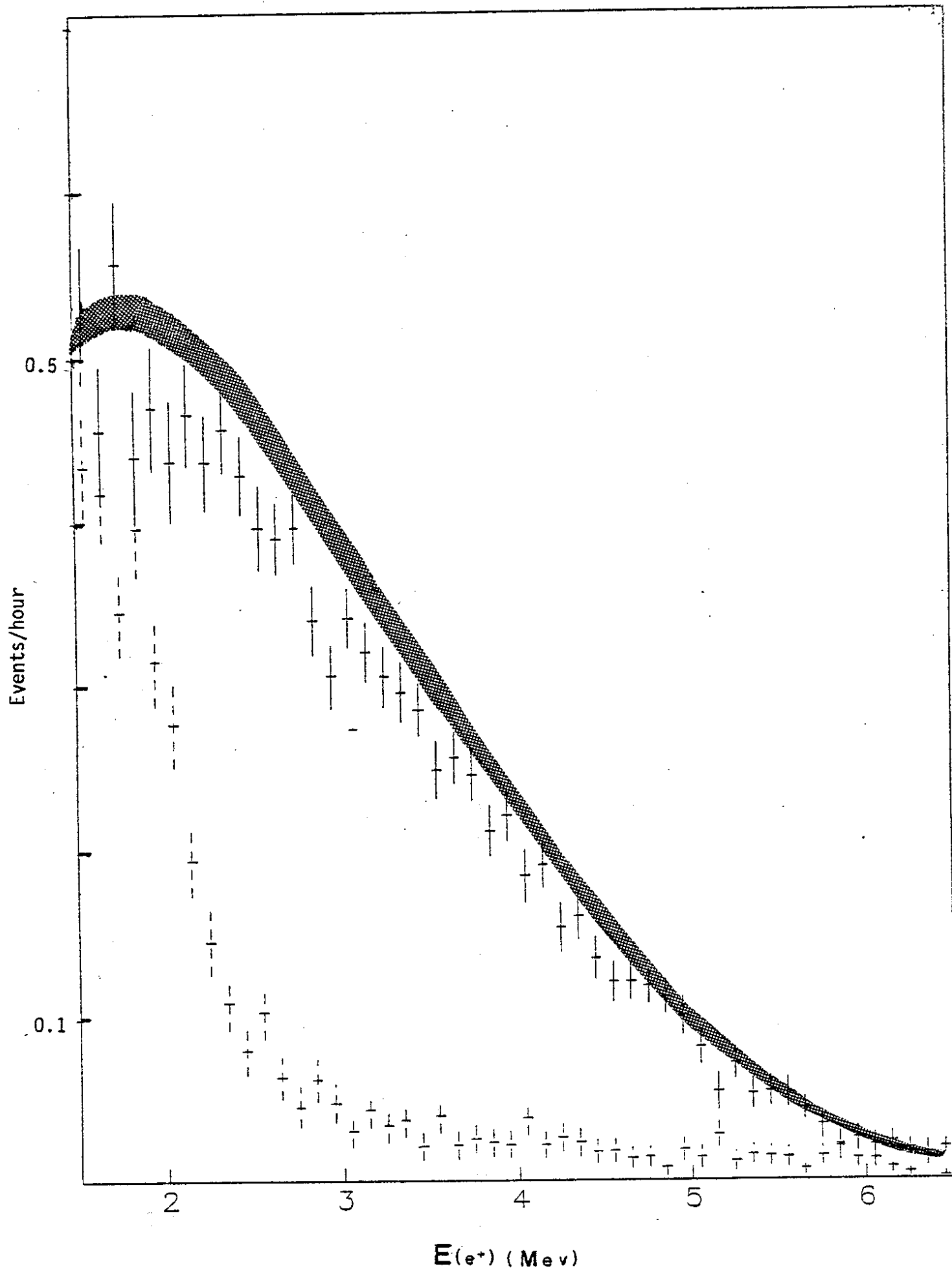
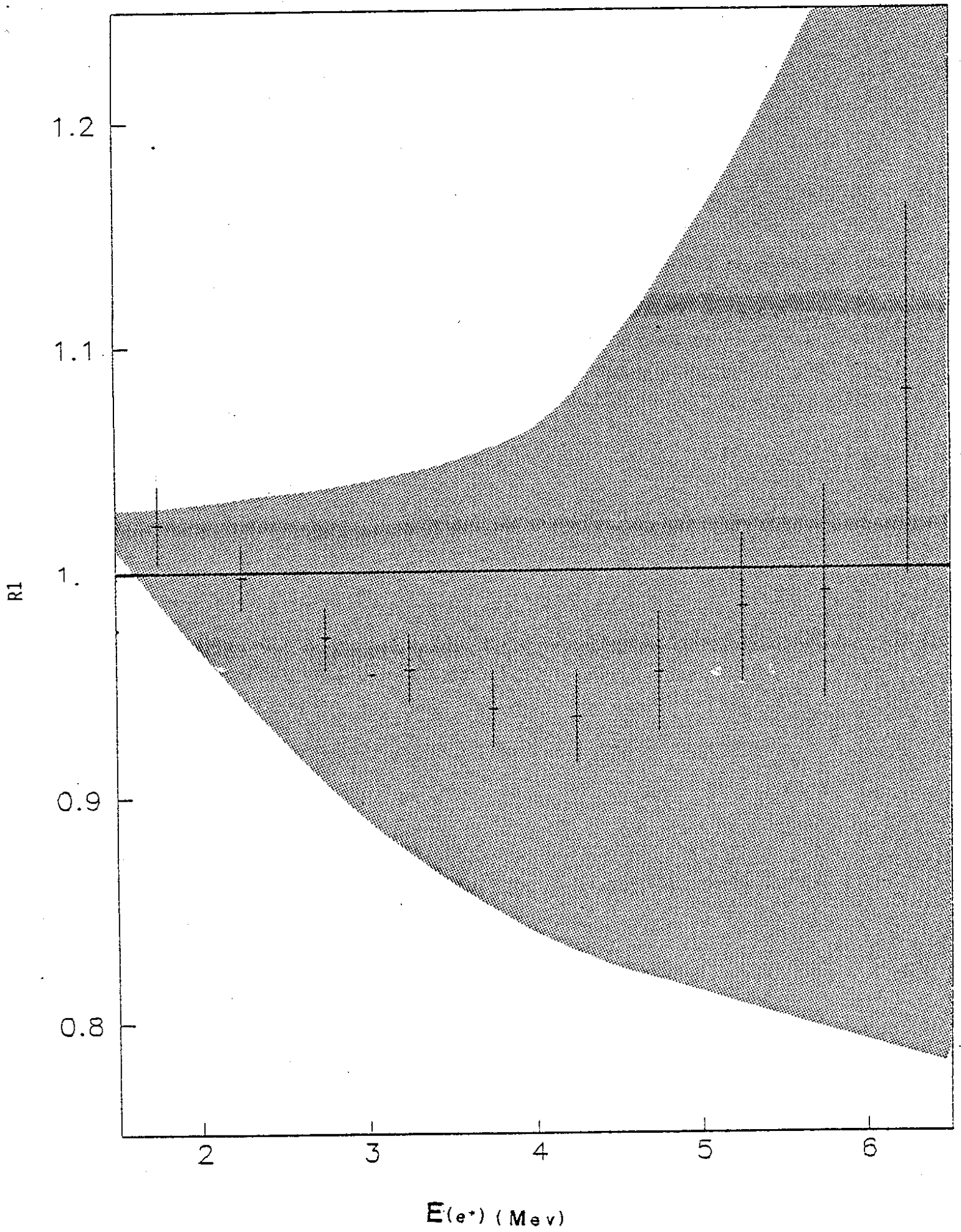


Figure 2B



$E(e^+) \text{ (MeV)}$

Figure 3A

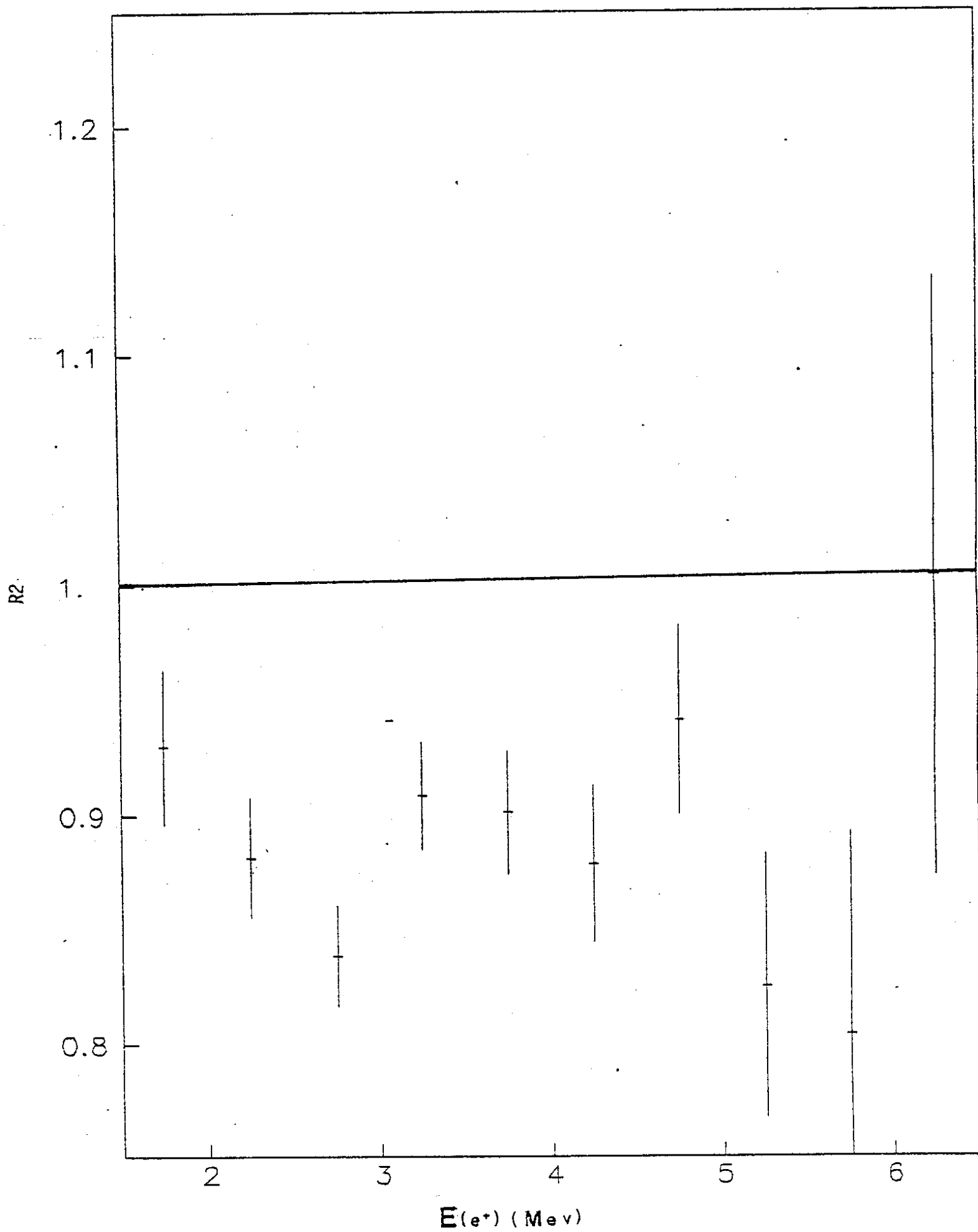


Figure 3B

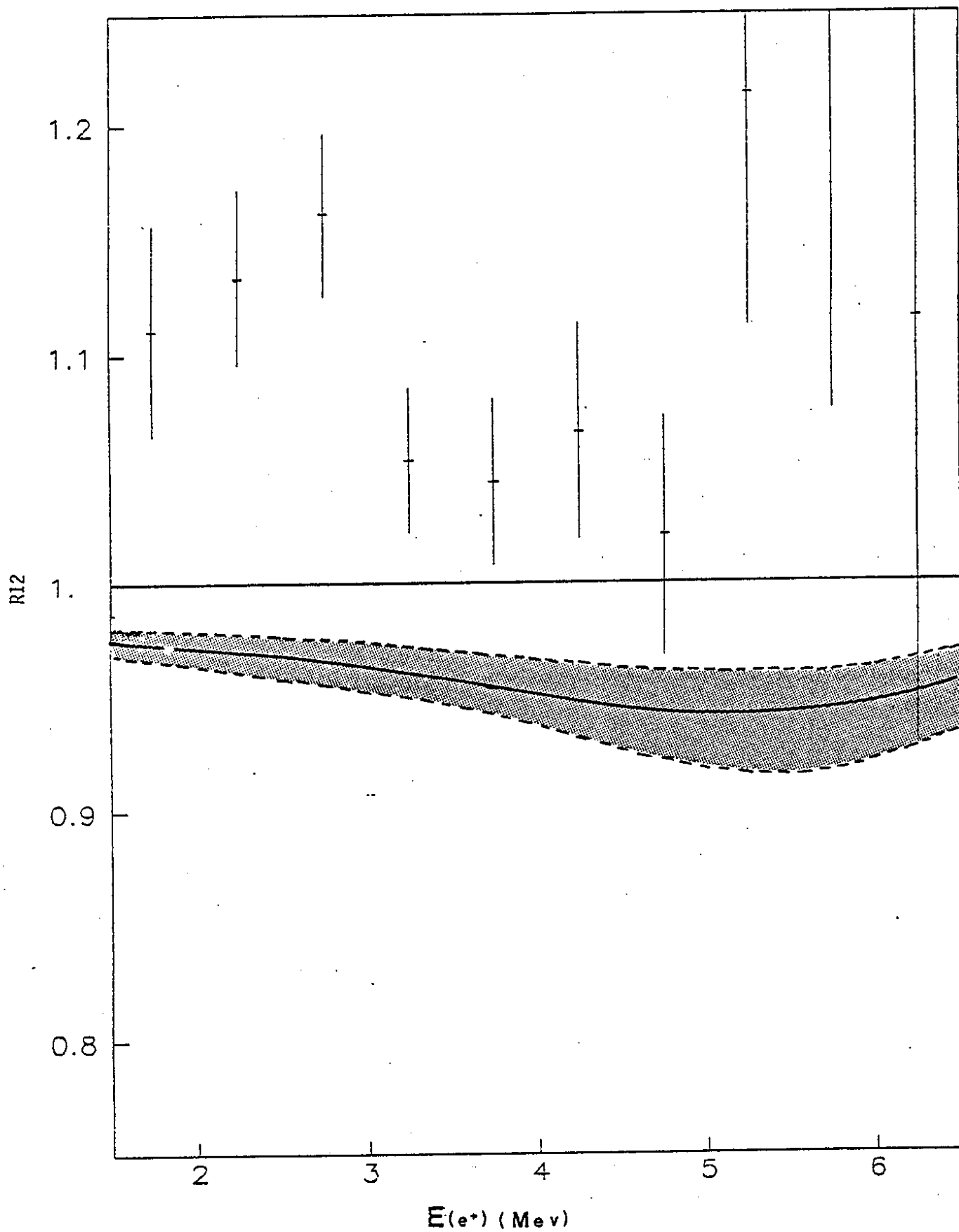


Figure 3C

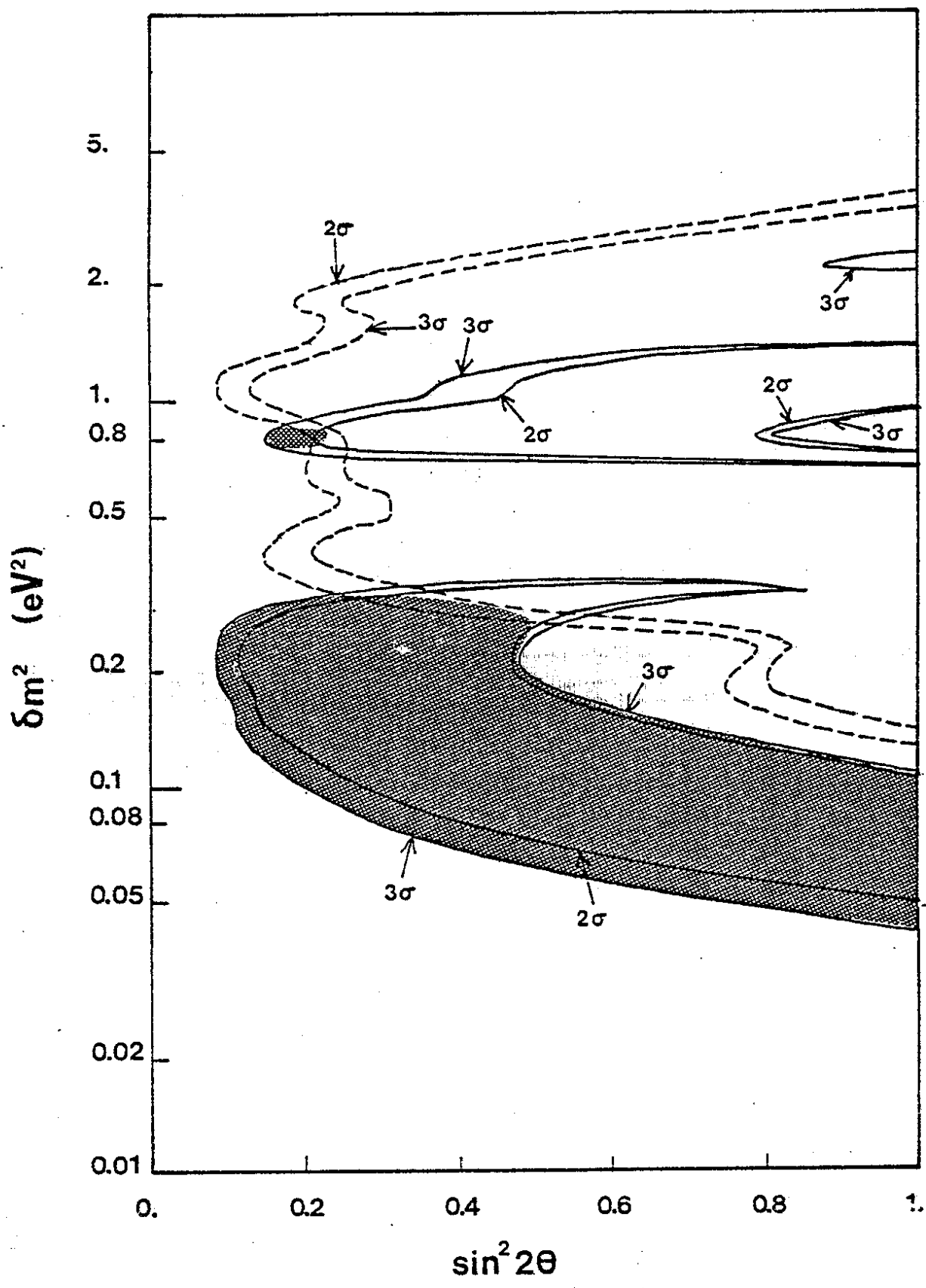


Figure 4